Moskal, L. M., K. Price, M. E. Jakubauskas and E. Martinko, 2001. Comparison of hyperspectral AVIRIS and Landsat TM imagery for estimating burn site pine seedling regeneration densities in the Central Plateau of Yellowstone National Park. In: *Proceedings of The 3rd International Forestry and Agriculture Remote Sensing Conference and Exhibition*, Denver, CO.

COMPARISON OF HYPERSPECTRAL AVIRIS AND LANDSAT TM IMAGERY FOR ESTIMATING BURN SITE PINE SEEDLING REGENERATION DENSITIES IN THE CENTRAL PLATEAU OF YELLOWSTONE NATIONAL PARK

Ludmila Monika Moskal
Kevin P. Price
Mark E. Jakubauskas
Kansas Applied Remote Sensing Program
and Department of Geography
moskal@ku.edu
price@ku.edu
mjakub@ku.edu

Edward A. Martinko
Kansas Applied Remote Sensing Program
and Department of Ecology and Evolutionary Biology
martinko@ku.edu

University of Kansas
Lawrence, KS 66045

ABSTRACT

Knowledge of seedling regeneration in burn sites is a valuable aspect of ecosystem monitoring. Remote sensing methods are ideal for such monitoring since large spatial extents can be monitored at multiple time scales. The goal of this project was to asses how well hyperspectral AVIRIS data can discriminate the differences between seedling densities in postfire regenerating sites, as compared to Landsat TM data. The field data were collected in the burn sites (legacies of the 1988 fires) of the Central Plateau, Yellowstone National Park during the summer of 1997. Timber cruising methods were used to count the seedlings at 24 sites. Other data reported included the basal area of the dead wood in the study plots. The project incorporated statistical methods (discriminant analysis), AVIRIS hyperspectral image and Landsat TM image classification and analysis methods (endmember selection/ evaluation and Spectral Angle Mapper classification). The statistical analysis showed that the hyperspectral imagery classified the seedling density classes with almost a 20 % improvement in accuracy compared to using only the Landsat TM imagery. This improvement was solemnly based on the hyperspectral content of the data, as the spatial variability was kept constant, by resampling the AVIRIS imagery to Landsat TM imagery resolution (30 m per pixel resolution). When the spatial content of the AVIRIS data were applied the improvement was close to 10 %, suggesting that the spatial information, summarized by a texture measurer, contributed additional information to the classification of seedling densities. Other relationships observed included the correlation between spectral and spatial data and the basal area of dead wood in the study plots. One of the future goals of this work is to incorporate multi-temporal analysis, where the rate in change of the density classes will be applied to determine the rate of regeneration of the stands.

1.0 INTRODUCTION

Fire is an important agent of change in an ecosystem. The large fires of 1988 in Yellowstone National Park demonstrated how dramatically and rapidly the vegetation and consequently the state of an ecosystem can change. The 250,000 ha of burnt forest created striking mosaic of burn severities on the landscape of the park. Both the ecological and economic impacts of these fires have been significant (YNP 1993; Polzin *et al.* 1993). The burns have begun to naturally regenerate with lodgepole pine (*Pinus contorta*) seedlings (Reed *et al.* 1999). The influence of this regeneration on ecological processes affecting the fauna of that ecosystem will have an impact for decades to come (Norland *et al.* 1996). For example, populations and movements of animals are directly and indirectly influenced by the vegetation present in their habitat (Boyce 1998 and 1997; Merrill *et al.* 1993; Boyce and Merrill 1991). Therefore, knowing where and how the burns are regenerating is an important aspect of sustainable park management strategies.

Monitoring the regeneration success through field methods is a daunting task involving large amounts of time and financial resources. However, new geospatial technologies, such as remote sensing, have made information collection available where field surveying has fallen short because of prohibiting factors such as cost, timing and terrain difficulties (Smith *et al*. 1990). The spatial extent of remotely sensed data as well as the temporal availability of such data are proving to be a very important tool in the task of accurate and timely forest inventory mapping and thusly, successful sustainable forest management. Since the early 1980's, the spectral information available from remote sensors has increased (Goetz *et al.* 1985), providing scientists with hyperspectral sensors such as the airborne AVIRIS, HyMap and *casi* or the satellite sensor Hyperion. In contrast to broadband remote sensing instruments (Landsat TM) which measure reflectance in only a few channels over broad wavelength regions, these imaging spectrometers measure light that has been reflected from the surface in numerous and continuous channels and suing narrow bandwidths. This ability to capture even subtle changes in the reflectance of the targets of interest is especially important in the study of vegetation (Vane and Goetz, 1993). Numerous studies have suggested ways to infer vegetation quantities such as biomass from remotely sensed imagery (Price *et al.* 1999; Dungan 1998; Teillet *et al*. 1997; Chen 1996; Jakubauskas 1996; Franklin *et al*. 1997; Franklin 1994; Hunt 1994; Tucker *et al.* 1991; Heute 1988; Running and Coughlan 1988; Running *et al.* 1986). Most take advantage of the high absorbance of vegetation in the red spectrum and the high reflectance in the near infrared that is captured by sensors such as Landsat TM. However, other vegetation characteristics such as canopy structure and leaf biochemistry are not as easily obtained from these spectrally broad sensors. Forest fire scientists, researchers and ecologists have been applying remotely sensed data to map and study fire effects (Rogan and Yool 2000), fire fuels (Root and van Wagtendonk 1999; Hawkes 1995) fire susceptibility (Uhl and Kauffman 1990) and postfire recovery (White *et al.* 1996), much of the research focused on coarse resolution sensors such as Landsat TM, however, little work has been done on the applicability of hyperspectral imagery.

The striking differences between information gathered by the Landsat TM sensor and the AVIRIS sensor is well demonstrated in Figure 1. The unique capability of the hyperspectral sensor to collect spectral information in numerous continuos channels and over a greater spectral range then the Landsat TM sensor provides the user with a more detailed spectral data of the target of interest. The additional information could prove to be a key in vegetation quality and quantity mapping and an applicable tool in monitoring forest fire regeneration.

The purpose of this study was to asses how well hyperspectral AVIRIS data would discriminate the differences between seedling densities in postfire regenerating sites, as compared to the Landsat TM data. Spatial information derived from 2nd order texture of the AVIRIS data were also evaluated for its seedling density classification potential.

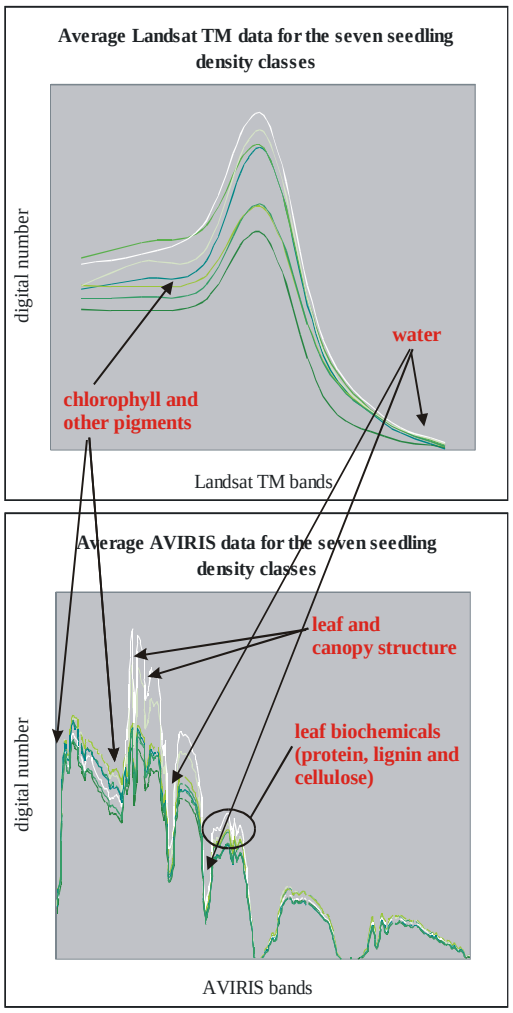

Figure 1. Generalized graphs of the seven seedling density classes, using Landsat TM data and AVIRIS data (based on Kokaly *et al.* 1998).

2.0 STUDY AREA

The Yellowstone National Park, the oldest park in the Unites States, located in the northwest corner of Wyoming encompasses about 9000 km^2 and is primarily a high, forested plateau. The climate in this region is generally cool with relatively moist springs and dry summers (Martner 1986). The vegetation of the plateau is controlled mainly by elevation, with moisture generally increasing with elevation, and the geological substrate likewise related to the soil formation (Despain 1990). The coniferous forest canopy of Yellowstone is dominated by lodgepole pine (*Pinus contorta*). However, older stands, approximately 250 to 350 years old comprise mostly of subalpine fir (*Abies lasiocarpa*) and Engelmann spruce (*Picea engelmanni*). Douglas fir *(Pseudosuga menziesii)* is also present in the region. Historically, fire was a common natural disturbance in the region, but when it was suppressed it lead to the

dramatic fires of 1988, which burned almost 45% of the park (Despain 1990). Romme and Despain (1989) have reported fires of such scale occurring in the past, most recently in the early 1700s. Our study was limited to the eastern part of the Central Plateau of Yellowstone National Park, do to the spatial extent of the AVIRIS imagery, shown in Figure 2.

3.0 METHODS

3.1 FIELD DATA

A fully random sampling method was utilized to collect field data in the postfire sites (legacies of the 1988 fires) during the summer of 1997. A fixed plot method of ground sampling (similar to methodology utilized by Franklin and McDermid (1993) was chosen for collecting field estimates of seedling densities for comparison to the remotely sensed data. The plots were located well within homogenous areas of the regenerating burns. Timber cruising methods were used to count the seedlings in twenty-four, 20 m by 20 m plots. Other data reported included the basal area of the dead wood in the plots.

Table 1. Seedling density classes based on the number of seedlings per hectare.

Class	Density (# of seedlings per hectare)
1	less then 500
2	1500
3	5000
4	20,000
5	40,000
6	100,000
7	greater then 100,000

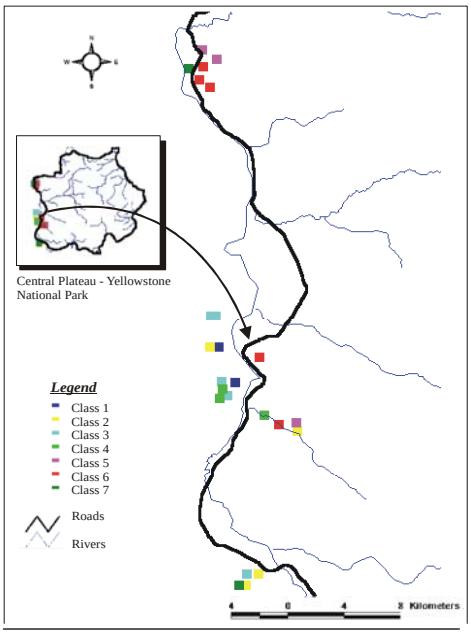

Figure 2. Location of field sites and seedling density class membership.

The field plots were grouped into seven classes, based on per hectare density of the regenerating burn sites. Not all-possible seedling regeneration densities were represented due to sampling constraints such as accessibility, spatial extent of the AVIRIS imagery and time limitations. The class break-up is shown in Table 1, and the locations of the sites and class groupings are illustrated in Figure 2. Class one consisted of plots without or very few seedlings; the 7th class grouped sites with vigorous seedling regeneration of over 100,000 seedlings per hectare. A stand representing moderate seedling regeneration is shown in Figure 3; also notable are the standing dead and fallen dead trees.

3.2 REMOTELY SENSED DATA

Two image data sets were applied in this study. The Airborne Visible and Infra-Red Imaging Spectrometer (AVIRIS) operated by NASA/JPL imagery was collected on July 14th 1997 and consisted of 224 image bands. AVIRIS collected the data in continuos channels of approximately 10 nanometers (nm) and the spectral wavelength range was from 350 to 2500 nm. The AVIRIS sensor collected 10.5-kilometer wide swath with an approximate 15 m per pixel resolution. The Landsat TM 5 scene was collected on July 18th, 1997 and consisted of 6 spectral bands.

The Landsat TM and the AVIRIS data were georectified and the AVIRIS images were merged to produce a spatially continuous data set. Raw DN of the Landsat TM and AVIRIS data were used in this project because atmospheric correction software for the AVIRIS data was not available at the time of the analysis. Because the two data sets were not used for direct comparisons but to test the same method of classification on each data set independently, the uncorrected data were deemed suitable for the purpose of this project.

The two image data sets were of different per pixel spatial resolutions. Hence, a filtering method (Jensen 1996) was used to reduce the spatial resolution of the AVIRIS data to match the 30-m per pixel resolution of the Landsat TM data. In doing so any differences in classifications results were attributed to the spectral content of the images and not the spatial content defined by image resolution.

The AVIRIS data set, at full spatial resolution (~15 m per pixel resolution), was used to produce 2nd order homogeneity texture, based on the equation below (Haralick *et al.* 1973). An average of bands in the near-infrared spectrum, which showed a high contrast for the seedling classes, was chosen as the band for the calculation of the texture measure. A fine three by three window size was used and all directions within the window were applied for the texture calculation.

Per pixel information was extracted for all of the seedling sites from the Landsat TM, the spatially resampled AVIRIS, the full resolution AVIRIS, and the textural data sets. The data were imported to the Statistical Products and Service Solutions (SPSS 1997) statistical package.

Figure 3. Example of one of the post 1998 fire regeneration sites with moderate pine seedling regeneration.

$$Homogeneity = \sum_{j=1}^{n}\sum_{i=1}^{m}\frac{P(i,j)}{(1+[R(i)-C(j)]^2)}$$

Where:
P(i,j) =the spatial co-occurrence matrix element
R(i) =the gray level value for a row and
C(j) =the gray level value for a column

3.3 DATA CLASSIFICATION

3.3.1 Discriminant Analysis

The classification decision rule selected for this study was the discriminant analysis function (Tabachnick and Fidell 1996). The procedure generated a set of discriminant functions based on linear combinations of the predictor variables (remotely sensed spectral bands for the AVIRIS and the Landsat TM sensors and spatial relationships summarized by the 2nd order texture) that provided the best discrimination between the seven seedling density groups. Three discriminant models were produced and included: a model using spectral Landsat TM data alone, a model using spatially resampled spectral AVIRIS data alone, and a model using a combination of the full resolution spectral AVIRIS data and 2nd order image texture. A stepwise discriminant analysis method was used for all three models where the critical F value for entry into the equation was set at 0.05 and the critical F for removal from the equation was set to 0.10.

3.3.2 Accuracy Assessment for the Discriminant Analysis

Congalton and Green (1998) suggest that at least 50 samples for each class or category should be used for accuracy assessment. Due to the limited seedling sample size the accuracies of the discriminant functions were tested using a *Jack-Knife Cross Validation* approach. The method was implemented by withholding the variables (spectral and/or textural) for one seedling site and building the discriminant function model using the information from the remaining seedling sites. The process of removing one seedling site from the dataset was repeated until all seedling sites had been withheld. Co-occurrence matrices were consequently calculated.

Producer and *User* classification accuracies, as suggested by Felix and Binney (1989), were reported for each co-occurrence matrix. The bottom row of each matrix shows the errors of omission known as the *Producer* classification accuracy. The Kappa coefficients of agreement represented by the K_{hat} statistic defined by Cohen (1960) and also described by Congalton and Green (1998) were used to score the actual agreement minus the chance agreement of a co-occurrence matrix and so further evaluate the classification accuracies.

3.3.3 Spectral Angle Mapper Classification (SAM)

In a final step, the Spectral Angle Mapper (SAM), a physically based classification that uses the n-dimensional angle to match pixels to reference spectra, was used to produce a classification map from the AVIRIS data (ENVI 1999). In this research the reference spectra were collected from the AVIRIS imagery for all seven-seedling density classes in the regenerating burn sites. Consequently, the field sites were used as endmembers for the classification. The ENVI algorithm, based on this theory, determined the spectral similarities between two spectra by calculating the angle between the spectra, treating the spectra as vectors in space with dimensionality equal to the number of bands in the AVIRIS imagery data set (ENVI 1999). All field sites were used to create the vectors and the accuracy of how well the classification performed was evaluated by determining how many pixels for each of the 24 field sites (delineated by a 3x3 window) were classified into the correct seedling density groups.

4.0 RESULTS AND DISCUSSION

4.1 COMPARISON OF LANDSAT TM AND AVIRIS DISCRIMINTANT ANALYSIS

The stepwise discriminant analysis functions built using the spectral information from the Landsat TM data relied heavily on the red and near-infrared image bands, hence, these bands were the first to enter the discriminant function model. This is consistent with other research where Landsat TM data was used for vegetation mapping (Price *et al.* 1999). The blue band showed no significant improvement to the model, with a critical F value of less then 0.10, hence, it was removed from the discriminant function. Atmospheric interference, which was not corrected for, in the blue band is much higher then in the near infrared bands, therefore explaining why the blue band was less useful in the analysis (Jensen 1996). The results of the stepwise method of discriminant analysis, in Table 2, showed that Landsat TM data preformed well for the low-density seedling classes, but confusion occurred between the moderate to high seedling density classes (classes 3 through 7). The results were highest for the 1500 seedlings per hectare class, where no errors of omission or commission occurred. Highest errors of omission and commission befell in the very high seedling density class (class 7). On average, the errors of omission and commission were 73.9% and 75.4%, respectively. The overall classification accuracy was about 75%. However, when the K_{hat} statistic was applied the classification accuracy was shown to be only about 58%.

Table 2. Error matrices derived from the discriminant analyses of the Landsat TM and AVIRIS data.

Discriminant analysis results for Landsat TM

	Seedling Density Class								*User's*
	1	***2***	***3***	***4***	***5***	***6***	***7***	***Tot***	***(commission)***
1	42	-	-	-	-	-	-	42	***100%***
2	-	63	-	-	-	-	-	63	***100%***
3	-	-	71	-	-	-	28	99	***72%***
4	21	-	-	48	-	-	-	69	***70%***
5	-	-	-	16	38	-	13	67	***57%***
6	-	-	21	-	-	84	-	105	***80%***
7	-	-	-	-	21	-	54	42	***50%***
Total	63	63	92	64	59	84	62		
(omission)									
Producer's	***80%***	***100%***	***77%***	***75%***	***55%***	***100%***	***34%***		

75 % of original grouped cases correctly classified (K_{hat} 58.44%)

Discriminant analysis results for resampled AVIRIS

	Seedling Density Class								*User's*
	1	***2***	***3***	***4***	***5***	***6***	***7***	***Tot***	***(commission)***
1	42	-	-	-	-	-	-	42	***100%***
2	-	42	21	-	-	-	-	63	***67%***
3	-	-	70	-	35	-	-	105	***67%***
4	-	-	-	63	-	-	-	63	***100%***
5	-	-	-	-	63	-	-	63	***100%***
6	-	-	-	-	-	71	34	105	***68%***
7	-	-	-	-	-	-	42	42	***100%***
Total	42	42	91	63	98	71	76		
(omission)									
Producer's	***100%***	***100%***	***77%***	***100%***	***64%***	***100%***	***55%***		

85.7% of original grouped cases correctly classified (K_{hat} 77.36%)

The stepwise discriminant analysis function built using the spectral information from the AVIRIS data also relied heavily on the red and near-infrared image bands, however, many of the bands in the 1 to 2.5 wavelength range also entered the discriminant function model. Some variables were removed from the analysis due to the high correlation between the bands. The results of the stepwise method of discriminant analysis, in the second part of Table 2, showed that AVIRIS data preformed well for the low-density seedling classes, the moderate and moderate to high density classes were classified correctly as well. Class three, the 5000 seedlings per hectare density class showed the greatest misclassification. The high (class 6) and very high (class 7) seedling density classes showed some misclassification due to the commission of 33% of the 7^{th} class to the to the 6^{th} class. This could be due to the presence of standing and fallen dead trees that contribute to the spectral signatures of the seedling study plots. Correlations between some of the AVIRIS bands and deadfall basal area were observed, but were not investigated in this project. On average, the errors of omission and commission were 85.2% and 85.9% respectively. The overall classification

accuracy was about 86%. However, when the K_{hat} statistic was applied the classification accuracy was shown to be about 77 %.

In comparison to the Landsat TM data the AVIRIS data showed an average improvement in classification accuracies of almost 20% and an average reduction of about 10% in the errors of omission and commission. Many of the misclassification errors in adjacent classes, as seen in the discriminant analysis of the Landsat TM data, were resolved in the discriminant analysis of the AVIRISI data.

4.2 DISCRIMINAT ANLSYSI USING AVIRIS AND TEXTURE

The results of the stepwise discriminant analysis functions built using the spectral information from the full 15 m per pixel resolution AVIRIS data and the homogeneity 2nd order image texture are shown in Table 3. AVIRIS based 2nd order homogeneity texture was not one of the first variables to enter the discriminant function model, however, it's improvement on the model was significant, increasing classification accuracies by almost 10%. All of the low density and moderate density seedling classes (from 1 to 5) were classified correctly. Suggesting that the spatial patterns of these classes captured by the texture derivative were responsible for the correct discrimination between the groups. The misclassification occurred between the two high (class 6) and very high (class7) seedling density classes due to the commission of 33% of the 7th class to the 6th class. These results suggest that there are no distinct spatial or spectral patterns between these two classes. On average, the errors of omission and commission were 93.5% and 95.4% respectively. The overall classification accuracy was about 95%. However, when the K_{hat} statistic was applied the classification accuracy was shown to be about 84%.

Table 3. The error matrix derived from the discriminant analysis of the AVIRIS data using full spatial resolution and implementing textural data.

Discriminant analysis results for AVIRIS data and texture based on full resolution AVIRIS

	Seedling Density Class								
	1	***2***	***3***	***4***	***5***	***6***	***7***	***Tot***	***User's (commission)***
1	42	-	-	-	-	-	-	42	***100%***
2	-	63	-	-	-	-	-	63	***100%***
3	-	-	105(100	-	-	-	-	105	***100%***
4	-	-	-	63	-	-	-	63	***100%***
5	-	-	-	-	63	-	-	63	***100%***
6	-	-	-	-	-	71	34	105	***68%***
7	-	-	-	-	-	-	42	42	***100%***
Total	42	63	105	63	63	71	76		
(omission)									
Producer's	***100%***	***100%***	***100%***	***100%***	***100%***	***100%***	***55%***		

95.2 % of original grouped cases correctly classified (K_{hat} 83.60%)

4.3 SPECTRAL ANGLE MAPPER CLASSIFICATION (SAM)

Seedling density map classified using the SAM method is shown in Figure 4. Out of the 24 plots represented by 216 pixels, 157 pixels were classified correctly. Therefore, the overall classification accuracy was 72.7% and the highest dispersion of the errors occurred in adjacent classes. The plots at the two extremes of the grouping scheme (very high seedling density and very low seedling density) had a classification accuracy of over 80%, but the middle classes (3 through to 6) had lower results.

The obvious problem with using the SAM classifier to only extract the seedling density endmembers was that image components in the AVIRIS data were classified into the seven seedling classes. The study area captured by the AVIRIS scene contained many different components, such as different type of forest stands, grasslands, clearings, roads, etc. Without attention to these classes, SAM did not perform to its optimum potential.

5.0 CONCLUSIONS

In most forestry applications seedlings or postfire regenerating areas are usually grouped into one class (Hudson, 1987), this research shows that a more detailed break-up of such class is possible, especially when hyperspectral data are available. The statistical analysis performed in this project showed the application of AVIRIS hyperspectral imagery to be an improvement in the discrimination of the seven seedlings density classes by almost 20 % as compared to the Landsat TM imagery. This improvement is solemnly based on the hyperspectral content of the AVIRIS imagery as the spatial resolution of the data sets was kept constant by resampling the AVIRIS imagery to Landsat TM imagery resolution. These results were encouraging, even without atmospheric correction of the data. However, atmospheric correction is still highly recommended (Gao and Goetz 1990). Because other image content, such as forested areas and the geyser basin, were not incorporated in the analysis the impact on the classification results by incorporating these classes is not known. The evidence that these classes play an important role in the dataset became clear when the SAM classification was preformed to produce a regeneration density map (Figure 4). The map was visually analysed, showing an overlap in the very low seedling areas and the geyser basin as well as in the forested areas and the very high seedling density class. One alternative approach to mapping the regenerating burn site seedling densities is to use a decision tree or two fold approach, where the burn sites or any regenerating areas (clearcuts) are first identified in the imagery through a classification procedure. Once the areas are delineated a second classification methods, using the field sites as endmembers can be used to classify the data into classes of increasing seedling regenerations densities. Another simpler approach is to use GIS vectors delineating the burn areas and limiting the analysis just to these regions, automation of this process could be based on methods my Franklin *et al.* (2000).

Spatial patterns of the seven seedling density classes captured by the 2nd order homogeneity texture derivative are responsible for a 10% improvement in classification accuracies. Similar results where texture was implemented have been reported by other researchers (Niemann *et al.* 1998; Jakubauskas 1997; Wulder *et al.* 1997; Marceau *et al.* 1990). Therefore, spatial information proved to be a useful tool in this application. Although this project did not evaluate different texture measurements such as other texture algorithms (entropy, etc.), various spatial extents (window sizes) and directions, it is clear that a classification approach that involves the inclusion of such data is highly recommended. Future work could address the texture measure most appropriate in this type of research.

The presence of dead trees, quantified by the basal area, has been observed to correlate with some of the hyperspectral bands. A large sample size stratified for various classes of dead tree basal area and seedling densities is a possible area of investigation in this type of research. Another area of investigation which would prove valuable in the interpretation of the hyperspectral AVIRIS imagery are ground collected spectra of the seedling density sites, to determine how unique these classes are, similar to work by Price (1994). Future goals of this project are to incorporate multi-temporal analysis of Landsat TM and/or hyperspectral images and ground data (see Price *et al.* 1992; 1993). In this future project the change of seedling counts based on field observations will be applied to determine the rate of regeneration of the stands based on yearly collected remotely sensed data.

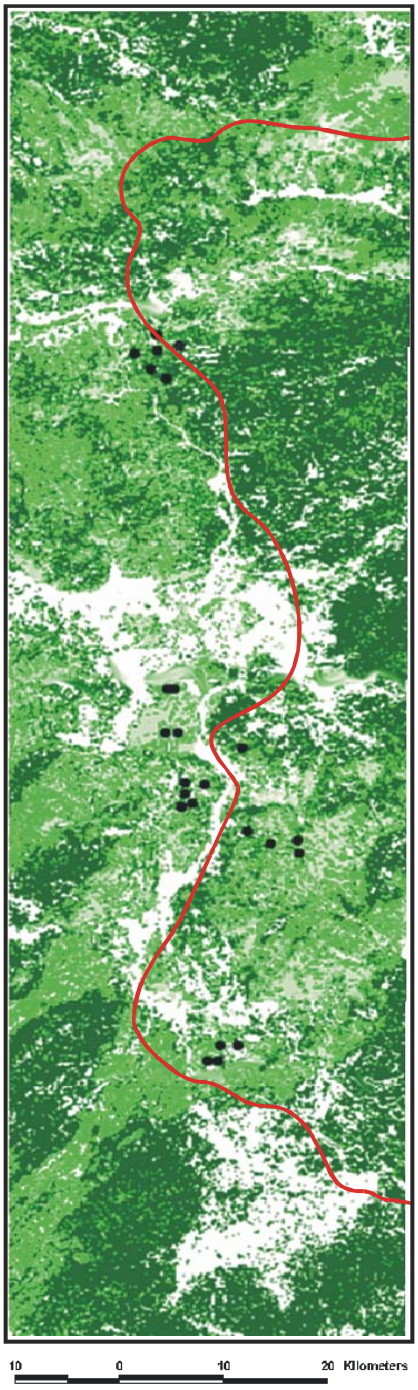

Figure 4. Postfire seedling density classification map using the SAM method and AVIRIS imagery. Map greenness increases with seedling density.

ACKNOWLEDGMENTS

This research was funded by the Natural Aeronautics and Space Administration, Earth Science Enterprise, under the Food and Fiber Applications of Remote Sensing (FFARS) Program, Grant Number NAS13-99019. This project was conducted at the Kansas Applied Remote Sensing (KARS) Program (Edward A. Martinko, Director).

6.0 REFERENCES

Boyce, M. S., 1998, Ecological-process management and ungulates: Yellowstone's conservation paradigm. *Wildl. Soc. Bull.* 26, 391-398.

Boyce, M. S., 1997, Review essay: The grizzly bears of Yellowstone. *Yellowstone Science* 5(1), 18-20.

Boyce, M. S. and E. H. Merrill, 1991, Ungulate responses to the 1988 fires in Yellowstone National Park. *Tall Timbers Fire Ecol. Proc.* 17, 121-132.

Chen, J.M., 1996, Evaluation of Vegetation Indices and a Modified Simple Ratio for Boreal Applications; *Can. J. of Rem. Sensing* , 22 (3), 229-242.

Cohen, J., 1960, A coefficient of agreement for nominal scales. *Education and Psychology Measurement*, 20(1), 37-46.

Congalton, R. G., and Green, K., 1998, *Assessing the Accuracy of Remotely Sensed Data: Principles and Practice*, CRC/Lewis Press, Boca Raton, FL.

Despain, D. 1990. Yellowstone Vegetation: Consequences of Environment and History in a Natural Setting. Roberts Rinehart Publishers, Santa Barbara.

Dungan, J., 1998, Spatial Prediction of Vegetation Quantities using ground and image data *Int. J. Rem. Sens.*, 19, 267-285.

ENVI, 1999, *3.2 Help System*, Research Systems Incorporated.

Felix, N. A., and Binney, D. L., 1989, Accuracy Assessment of a Landsat-assisted Vegetation Map of the Costal Plain of the Arctic National Wildlife Refuge. *Photogram. Eng. & Rem. Sens.*, 55(4), 475-478.

Franklin, S. E., T. M. McCaffrey, M. B. Lavigne, M. A. Wulder, and L. M. Moskal. 2000; An Arc/Info Macro Language (AML) Polygon Update Program (PUP) integrating forest inventory and remotely-sensed data, *Can. J. of Rem. Sens.*, 26, (6), 566-575.

Franklin, S., M. Lavigne, M. Deuling, M. Wulder, and E. Hunt, 1997; Estimation of forest leaf area index using remote sensing and GIS data for modeling net primary production, *Int. J. Rem. Sens.*, 18, (16), 3459-3471.

Franklin, S. E., 1994, Discrimination of subalpine forest species and canopy density using digital *casi*, SPOT and Landsat TM data, in *Photogram. Eng. & Rem. Sens.*, 60 (10), 11233-1241.

Franklin, S.E. and G. McDermid, 1993, Empirical relations between digital SPOT HRV and *casi* imagery and lodgepole pine forest stand parameters. *Int. J. Rem. Sens.*, 14, 2331-2348.

Gao, B. and Gotez, A. F. H., 1990, Column atmospheric water vapor and vegetation liquid ware retrievals from airborne imaging spectrometer data, *J. of Geophysical Research* 95(D4), 3549-3564.

Goetz, A. F. H, G. Vane, J. E. Solomon and B. N. Rock, 1985, Imaging spectrometry for earth remote sensing, *Science*, 228, 1147-1153.

Haralick, R.M., K. Shanmungam and I. Dinstein, 1973. Textural features for image classification. *IEEE Transactions on systems, man and cybernetics 3*, 610-621.

Hawkes, B., D. Goodenough, B. Lawson, A. Thomson, W. Sahle, K.O. Niemann, P. Fuslem, J. Beck, B. Bell, and P. Symington, 1995, Forest fire fuel mapping using GIS and remote sensing in British Columbia. *Summaries of the GIS'95*, Vancouver1995.

Heute, A. R., 1988. A Soil-Adjusted Vegetation Index (SAVI), *Rem. Sens. Env.*, 25, 295-309.

Hudson, W. D.,1987, Evaluation of Several Classification Schemes for Mapping Forest Cover Types in Michigan. *Int. J. Rem. Sens.*, 8, (12), 1785-1796.

Hunt, E.R. Jr, 1994, Relationship between woody biomass and PAR conversion efficiency for estimating net primary production from NDVI. *Int. J. Rem. Sens.*, 15:1725-1730.

Jakubauskas, M.E. 1997. Effects of forest regeneration on texture in Landsat Thematic Mapper imagery. *Can. J. Rem. Sens.*, 23(3):251-257.

Jakubauskas, M.E. 1996. Canonical correlation analysis of coniferous forest spectral and biotic relationships. *Int. J. Rem. Sens.*, 17(12):2323-2332.

Jensen, J. R. 1996. *Introductory Digital Image Processing. A Remote Sensing Perspective*, Simon & Schuster, Upper Saddle River, N.J.

Kokaly, R. F., R. N. Clark, and K. E. Livo, 1998, Mapping the Biology and Mineralogy of Yellowstone National Park using Imaging Spectroscopy, *Summaries of the 7th Annual JPL Airborne Earth Science Workshop*, R.O. Green, Ed., JPL Publication 97-21. Vol. 1, AVIRIS Workshop, conducted Jan 12-16, 1998, 245-254.

Marceau, D. J., Howarth, P. J., Dubois, J. M. M., and Gratton, D. J., 1990, Evaluation of the gray-level co-occurrence matrix method for land-cover classification using SPOT imagery. *IEEE Transactions on Geoscience and Remote Sensing*, 28(4), 513-518.

Marther, B. E., 1986, Wyoming climate atlas. Lincoln: University of Nebraska Press.

Merrill, E. H., R. W. Marrs, M. B. Brodahl, and M. S. Boyce, 1993, Estimations of green herbaceous phytomass in Yellowstone National Park using remote sensing, *J. Range Manage*. 46, 151-157.

Niemann, K.O., D.G. Goodenough, D. Marceau, and G. Hay, 1998, A practical alternative for fusion of hyperspectral data with high resolution imagery. *Proceedings of the IGARSS'98* Seattle.

Norland, J.E., F.J. Singer, L. Mack. 1996. Effects of the Yellowstone fires of 1988 on elk habitats. 223-232, in: *Ecological implications of fire in greater Yellowstone. International Ass. Wildland Fire*, Fairfield, WA.

Polzin, P.E., M.S. Yuan and E. G. Schuster, 1993. *Some economic impacts of the 1988 fires in the Yellowstone area. United States Department of Agriculture*, Forest Service, Intermountain Research Station, Research Note INT-418.

Price, J. C., 1994, How Unique are Spectral Signatures. *Rem. Sens. Env.*, 49, 181-186.

Price, K. P, X. Guo and J.M. Stiles, 1999, Discriminant analysis of Landsat TM multi-temporal data for six grassland management practices in eastern Kansas, *Proceedings of the ASPRS 1999 Annual Convention*, Portland, Oregon, 498-508.

Price, K. P., V.C. Varner, E. A. Martinko, D. C. Rundquist, and J. S. Peake. 1993. Influences on land management and weather on plant biophysical and hyper-spectral response patterns of tallgrass prairies in northeastern Kansas. *Proceedings of the PECORA12 Conference*, Sioux Falls, South Dakota, August 24-26.

Price, K. P., V. C. Varner, E. A. Martinko, and D. C. Rundquist. 1992. Analysis of multitemporal narrow-band spectroradiometer measurements from six prairie treatments in Kansas. *Proceedings of the ASPRS/ACSM '92 Annual Convention*, Albuquerque, New Mexico.

Reed, R. A., M. E. Finley, W. H. Romme and M. G. Turner, 1999, Aboveground net primary production and leaf area index in early postfire vegetation in Yellowstone National Park, *Ecosystems*, 2, 88-94.

Rogan, J. and Yool, S.R. 2000, Mapping fire-induced vegetation depletion in the Peloncillo Mountains, Arizona and New Mexico. *Int. J. Remote Sens.*

Romme, W.H. and D.G. Despain, 1989, Historical perspective on the Yellowstone Fires of 1988. *Bioscience*, 39(10), 696-699.

Root, R. R., and J. W. van Wagtendonk. 1999. Hyperspectral analysis of multi-temporal Landsat TM data for mapping fuels in Yosemite National Park. *Proceedings of the Annual Conf. Amer. Soc. Photog. and Remote Sensing.* Portland, OR.

Running, S. W., and J.C. Coughlan: 1988. "A General Model of Forest Ecosystem Processes for Regional Applications". I: Hydrologic Balance, Canopy Gas Exchange and Primary Production Processes, *Ecol. Model.* 42, 125-154.

Running, S. W., Peterson, D. L., Spanner, M. A., and Teuber, K., 1986, Remote Sensing of coniferous forest leaf area. *Ecology*, 67(1), 273-276.

Small, C., 1999, Estimation of Vegetation Abundance by Linear Spectral Unmixing, Submitted for Publication.

Smith, O., M., Ustin, L., S., Adams, B., J., and Gillespie, R., A., 1990, Vegetation in Deserts: I. A Regional Measure of Abundance from Multispectral Images, *Rem. Sens. Env.*, 31:1-26.

SPSS, 1997, *SPSS Base 7.5 for Windows User's Guide*, SPSS Inc.

Tabachnick, B. G., and Fidell, L. S.,1996, *Using Multivariate Statistics*, Harper Collins College Publishers, California State University, Northridge.

Teillet, P. M., K. Staenz K. and D. Williams D., 1997, Effects of Spectral, Spatial, and Radiometric Characteristics on Remote Sensing Vegetation Indices for Forested Regions; *Rem. Sens. Env.*, 61 ,139-149.

Tucker, C.J., W.W. Newcomb, S.O. Los, and S.D. Prince, 1991: Mean and inter-year variation of growing season normalized difference vegetation index for the Sahel 1981-1989. *Int. J. Rem. Sens.*, 12, 1133-1135.

Uhl, C., and J.B. Kauffman. 1990. Deforestation, fire susceptibility, and potential tree responses to fire in the eastern Amazon. *Ecology* 71, 437-449.

Vane, G., and A. Goetz, 1993, Terrestrial imaging spectrometry: Current status, future trends, *Rem. Sens. Env.*, 44, 117-126.

White, J.D., K.C. Ryan, C.C. Key, S.W. Running. 1996. Remote sensing of forest fire severity and vegetation recovery. *Int. J. of Wildland Fire*, 6 (3), 125-136.

Wulder, M. A., Lavigne, M. B., LeDrew, E. F., and Franklin, S. E., 1997, Comparison of Texture Algorithms of LAI: first-order, second-order, and semivariance moment texture (SMT). *Proceedings of the 19th Canadian Remote Sensing Symposium*, Ottawa, Ontario.

YNP, 1993, *The ecological implications of fire in Greater Yellowstone: second biennial scientific conference on the Greater Yellowstone Ecosystem*, September 19-21, 1993, Mammoth Hot Springs, Yellowstone National Park.